Physica Scripta

PAPER

Retardation theory of eleven galaxies

Michal Wagman[1], Lawrence Paul Horwitz[1,2,3] and Asher Yahalom[4,5,*]

[1] Department of Physics, Ariel University, Ariel 40700, Israel
[2] School of Physics, Tel Aviv University, Ramat Aviv 69978, Israel
[3] Department of Physics, Bar Ilan University, Ramat Gan 52900, Israel
[4] Faculty of Engineering, Ariel University, Ariel 40700, Israel
[5] Princeton University, Princeton, NJ 08543, United States of America
[*] Author to whom any correspondence should be addressed.

E-mail: mwgman@gmail.com, larry@tauex.tau.ac.il and asya@ariel.ac.il

Keywords: general relativity, dark matter problem, galactic dynamics

OPEN ACCESS

RECEIVED
3 March 2024

REVISED
18 July 2024

ACCEPTED FOR PUBLICATION
7 August 2024

PUBLISHED
2 September 2024

Abstract

The missing mass problem has been with us since the 1970s, as Newtonian gravity using baryonic mass cannot account for various observations. We investigate the viability of retardation theory, an alternative to the Dark Matter paradigm (DM) which does not seek to modify the General Principal of Relativity but to improve solutions within it by exploring its weak field approximation to solve the said problem in a galactic context. This approach have yielded satisfactory results, with respect to galactic rotation curves, the Tully-Fisher relation and missing mass derived from gravitational lensing. Recently it was able to introduce a necessary correction to the virial theorem explaining mass excess in clusters of galaxies. The current work presents eleven rotation curves calculated using Retardation Theory. The calculated rotation curves are compared with observed rotation curves. Values for the change in mass flux to mass ratio are extracted from the fitting process as a free fitting parameter. Those quantities are interpreted here and in previous works using galactic processes. Retardation Theory was able to successfully reproduce rotation curves and a preliminary correlation with star birthrate index is seen, suggesting a possible link between galactic winds and observed rotation curves. Retardation Theory shows promising results within current observations. More research is needed to elucidate the suggested mechanism and the processes which contribute to it. Galactic mass outflows carried by galactic winds may affect rotation curves.

1. Introduction

From an empirical perspective general relativity (GR) is known to be verified by many different types of observations [1–5]. However, currently Einstein's general relativity is at a rather difficult position. It has much support from observational evidence while also having serious challenges. The observational verifications it has gained in both cosmology and astrophysics are in doubt due to the fact that it needs to include unconfirmed ingredients, dark matter and energy, in order to achieve successes on the larger scales of galaxies, clusters of galaxies and universe as a whole. In most cases the unconfirmed ingredient is used while at the same time practitioners neglect a major ingredient of general relativity, the phenomenon of retardation, that negates Newtonian action at a distance.

Indeed, the so called dark matter enigma has troubled the astronomical community as early as the 1930s (or perhaps even as early as the 1920s then denoted as the question of missing mass). Additional dark matter (that is neglect of retardation effects) has been postulated on increased distances as those scales were scrutinized. A very detailed and costly forty-years underground and accelerator search was unsuccessful to provide evidence regarding its reality. The dark matter enigma is problematic as in recent years as the Large Hadron Collider failed to provide evidence for super symmetric particles, an essential ingredient that string theory needs, and it is that same string theory that is expected to quantize gravity.

As early as 1933, Zwicky noted that some galaxies located in the Comma Cluster have velocities significantly larger with respect to the velocities derived form virial calculations based on Newtonian paradigm [6, 7]. He derived that the mass required to facilitate the observed velocities is about 400 times larger than that of luminous matter (this was later mitigated somewhat). Of course, if Zwicky would have use the retarded gravity version of the virial theorem [8] no significant problem would arise. In 1959, on a smaller galactic scale, Volders observed that stars at large distances from the center of the Galaxy M33 do not move as they should [9]. That is to say that the velocities do not reduce proportionally to the inverse of the square root of the distance from the center.

The discrepancy is further corroborated in later years. Rubin & Ford [10, 11] have shown that many galaxies of spiral form the speeds at the external part do not reduce. Instead they attain a flat curve (or continue increasing) at a speed unique to every galaxy. It was demonstrated that the velocity curves can be derived from GR if one does neglect time dependence and the finite speed of propagation of gravity. The detailed analysis is given in [12–19]. The mechanism is strongly connected to the dynamics of the density of matter inside the Galaxy, or more specifically to the densities' second derivative. The density can change due to the depletion of gas in the galaxies surrounding (in which case the second derivative of the galaxies' total mass is negative [17]) but can also be affected by dynamical processes involving star formation and supernovae explosions [15, 16]. It was determined that all possible processes can be captured by three different length scales: the typical length associated with the spatial change of density, also the typical length associated with the spatial change of the velocity field and also the dynamical length scale. It is the shortest among those length scales that determine the significance of retardation [20].

The famous relation of Tully and Fisher [21] connecting the luminous matter of a galaxy to its rim speed in the fourth power is deduced from the finite propagation speed of gravity [22].

Retarded gravity does not affect only slowly moving particles but also photons. Although the mathematical analysis is slightly different in both cases [20, 23]. The analysis shows that the 'missing mass' is exactly the same in gravitational lensing as in rotation curves.

While the 'dark matter' assumption may still prevail, current status is sufficiently alarming to contemplate that this prevailing ideas should be reconsidered. We mention a few difficulties that add doubt to this common idea:

First, in order to comply with said observations and structure formation simulations a list of properties has been attributed to DM [7], which will not be listed here. However, to date, 50 years since its inception, DM has not been observed nor could any known particles be identified with its properties.

Second, dark matter simulations are notorious for having a core-cusp problem. Navarro-Frenk-White (NFW) [24] is the prevalent missing matter profile used today to describe galactic velocity curves and is derived from Cold Dark Matter computer calculations. However, NFW is not very successful, in particular for galaxies of the Low Surface Brightness type. Its consequences for galactic speeds and velocities derived from observations do not match. To be specific, NFW implies a 'cuspy' central domain for a 'missing mass' halo. By this it is meant that the inner density of the 'missing mass' is changing spatially fast. On the other hand observations suggest a 'core-like' (approximately the same density) distribution. Of course, many attempts have been made to solve this difficulty, but without success. In particular, solutions required more ad hoc paradigms and additional free parameters, and one could not avoid the deduction that those were introduced to artificially uphold a false assumption.

Third, the law of Sancisi's [25] is a significant empirical deduction. It challenges dark halos of many types. The content of the law is 'each and every property of the luminous matter distribution there is a corresponding indication in the velocity profile curve and vice versa'. To put this in different words, minute changes in the luminous matter profile ('features') are identified in the rotation curve. This is unexpected from a 'missing mass' paradigm: the dark halo is extremely massive with respect to baryonic matter according to standard modelling than the baryons. It thus follows that in prevalent areas of the Galaxy, small disturbances in the baryonic density are of no consequence to the rotational curve which contradict empirical data. The deviation between dark matter theory and observations in LSBs is much more severe. For LSBs the dark halo mass is much greater than luminous matter in every radius. However, in reality the rotation curve attests to every small baryonic change of mass distribution. Thus there is indeed room for the present suggestion.

Relevant literature on alternative theories to DM is specified in the following references: for Milgrom's MOND see [26], for Mannheim's Conformal Gravity see [27, 28], for Moffat's MOG [29]. In contrast to those previous alternative theories we adhere strictly to Occam's razor, as suggested by Newton and Einstein, replacing 'missing mass' with derivations inherent to GR, and in fact are hardwired within GR foundations. Notice, however, that the connection between retardation and MOND was recently elucidated [30], showing in what sense low acceleration MOND criteria can be derived from retardation theory and how MOND interpolation function can be a good approximation to retarded gravity. This will also be discussed briefly in the current paper.

We emphasize that appreciable retardation effects do not require that speeds of matter in the Galaxy are high (although this may help), in fact the vast majority of galactic bodies (stars, gas) are slow with respect to the speed

of light. In other words, the ratio of $\frac{v}{c} \ll 1$. Typical velocities in galaxies are 100 km/s, which makes this ratio 0.001 or smaller. To obtain appreciable retardation effects what is needed is a small typical gradient scale with respect to the size of the system [20]. It was shown that retardation effects may become significant even at low speeds, provided that the distance over a typical length scale is large enough.

Within the solar system retardation effects are not appreciable [31, 32]. However, galaxies' velocity curves indicate that the retardation effects cannot be neglected beyond a certain distance [15–17]. The purpose of this study is to establish the empirical basis for the retarded gravity theory. It expands previous work analysing eleven galaxies [16] and is thus a follow up from reference [16]. We show that in most cases we obtain an excellent fit without postulating dark matter or modifying general relativity.

2. Retardation effects beyond the newtonian approximation

The mathematical similarities between GR and Electromagnetic (EM) theory have not gone unnoticed. While exact solutions of GR have proven challenging due to the non-linear nature of the Einstein equations, within the weak field approximation the equations are linear, therefore superposable, yielding a Retarded Potential [3, 33] similar to that of EM theory [34, 35]. The form of the equations in both cases is related to the structure of the constant Lorentzian metric [36, 37].

Thus the retarded gravitational potential ϕ is given in equation (21) of [17]:

$$\phi = -G\int \frac{\rho\left(\vec{x}',\, t-\frac{R}{c}\right)}{R} d^3x' \tag{1}$$

The notations used are the same as in [17] and will not be redefined here.

When studying far field approximations of the Retarded Potential depicted in equation (1), in a way that resembles electromagnetism, the interesting possibility of gravitational waves has been deduced [3, 33]. For a century, the community has considered the possibility of Gravitational Waves, which have finally been observed [38] in the last decade with great excitement, and a new way of observing the Universe became possible. Since the far field approximation is not suitable for galaxies, as the Galaxy is the source system, retardation theory [12, 14, 17–20, 22, 23] studies a near field approximation.

Using equation (1) we may derive the force per unit mass:

$$\begin{aligned}
\vec{F} &= -\vec{\nabla}\phi = \vec{F}_{Nr} + \vec{F}_r \\
\vec{F}_{Nr} &= -G\int \frac{\rho\left(\vec{x}',\, t-\frac{R}{c}\right)}{R^2}\hat{R}d^3x', \qquad \hat{R} \equiv \frac{\vec{R}}{R} \\
\vec{F}_r &\equiv -\frac{G}{c}\int \frac{\rho^{(1)}\left(\vec{x}',\, t-\frac{R}{c}\right)}{R}\hat{R}d^3x', \qquad \rho^{(n)} \equiv \frac{\partial^n \rho}{\partial t^n}.
\end{aligned} \tag{2}$$

Thus a retarded potential does not simply imply a retarded Newtonian force $\vec{F}_{Nr}$, but in addition a pure 'retardation' force $\vec{F}_r$ which decreases more slowly than the Newtonian force with radius, thus deriving the unique shape of speed profiles of galaxies. It should be pointed out that the force spatial properties are not dependent on any type of expansion or approximation depending on the smallness of the delay time $\frac{R}{c}$ [17]. Notice, however, that the expansion does elucidate the force terms as we explain below.

$\frac{R}{c}$ is about 10^4 years, but may be smaller in comparison to the typical temporal intervals for which the baryonic density is modified. We thus may introduce a Taylor expansion:

$$\rho\left(\vec{x}',\, t-\frac{R}{c}\right) = \sum_{n=0}^{\infty}\frac{1}{n!}\rho^{(n)}(\vec{x}',\, t)\left(-\frac{R}{c}\right)^n. \tag{3}$$

Considering equations (3) and equation (1), we may write:

$$\begin{aligned}
\phi &= \phi_2 + \phi_{(n>2)} \\
\phi_2 &= -G\int \frac{\rho(\vec{x}',\, t)}{R}d^3x' + \frac{G}{c}\int \rho^{(1)}(\vec{x}',\, t)d^3x' - \frac{G}{2c^2}\int R\rho^{(2)}(\vec{x}',\, t)d^3x' \\
\phi_{(n>2)} &= -G\sum_{n=3}^{\infty}\frac{(-1)^n}{n!c^n}\int R^{n-1}\rho^{(n)}(\vec{x}',\, t)d^3x'
\end{aligned} \tag{4}$$

The first term is clearly Newtonian, the second expression if of no consequence as it does not depend on $\vec{R}$ or $\vec{x}$, the third expression is a correction to the Newtonian theory:

$$\phi_r = -\frac{G}{2c^2}\int R\rho^{(2)}(\vec{x}',\, t)\, d^3x' \tag{5}$$

Equation (4) describes a Taylor expansion, and thus is only applicable for a limited distance specified by the infinite sum convergence:

$$R < c\ T_{\max} \equiv R_{\max} \tag{6}$$

It thus follows that the approximation is only valid in the near field, this is to be compared with the different far field methodology of gravitational radiation [1, 39, 40]. The applicability of the formula is much limited when a second order expansion is considered [17].

Provided that the $n > 2$ terms are ignored, the force which is applicable to a unit mass can be written as:

$$\begin{aligned}
&\vec{F} \simeq \vec{F}_N + \vec{F}_{ar} \\
&\vec{F}_N = -\vec{\nabla}\phi_N = -G\int \frac{\rho(\vec{x}',\, t)}{R^2}\hat{R}d^3x', \qquad \hat{R} \equiv \frac{\vec{R}}{R} \\
&\vec{F}_{ar} \equiv -\vec{\nabla}\phi_r = \frac{G}{2c^2}\int \rho^{(2)}(\vec{x}',\, t)\hat{R}d^3x'.
\end{aligned} \tag{7}$$

$\vec{F}_N$ is purely Newtonian (no retardation) please see [18] for additional details. The insignificance of the term proportional $\frac{1}{c}$ is quite remarkable and also happens in the corresponding electromagnetic problem [41]. If $r = |\vec{x}| \to \infty$, it follows that: $\hat{R} \simeq \frac{\vec{x}}{|\vec{x}|} \equiv \hat{r}$; and also:

$$\vec{F}_{ar} = \frac{G}{2c^2}\hat{r}\int \rho^{(2)}(\vec{x}',\, t)d^3x' = \frac{G}{2c^2}\hat{r}\ddot{M}, \qquad \ddot{M} \equiv \frac{d^2M}{dt^2}. \tag{8}$$

The above approximation is rather useful as dominant retardation effect occur usually outside the main mass of the Galaxy. Generically a galaxy would apply an attractive force on intergalactic gas, its mass would thus increase so $\dot{M} > 0$; now since the intergalactic gas is reduced in mass, it is plausible that the speed at which the galactic mass is increased, must decrease and therefore $\ddot{M} < 0$. This is of course a much oversimplified description of the overall situation in which star formation and supernovae explosions affect the mass accretion rate of the Galaxy.

We may thus write:

$$\vec{F}_{ar} = -\frac{G}{2c^2}|\ddot{M}|\hat{r} \tag{9}$$

and the force due to retardation must be towards the galactic center (increased gravity).

$\vec{F}_N$ first introduced by Newton is attractive, however, the retardation force $\vec{F}_r$ may push or pull. Newton's force is proportional to $\frac{1}{R^2}$, in contrast, the force implied by retardation is not a function of radial distance provided the approximation of equation (3) is valid. For short distances, Newtonian forces surely are greater, however, for far radial distances the retardation force is bound to win. The Newtonian force is negligible for huge distances compared to the distance:

$$R \gg R_r \equiv c\Delta t \tag{10}$$

Δt is associated with the temporal second order derivative of ρ. For $R \ll R_r$, retardation can be neglected and only Newtonian forces need to be considered; this is the situation in the solar system. For the outer parts of galaxies neither force seems to be negligible, and both have to be considered.

Since for a typical galaxy $\ddot{M} < 0$ and a systems total mass is conserved, it follows that $\ddot{M} > 0$ for the intergalactic gas and thus $\vec{F}_{ar}$ in the Galaxy and out side the Galaxy should cancel each other. Notice, that this argument is incorrect because equation (7) is only valid when $\frac{R}{c}$ can be considered diminutive, it is not diminutive if all the Universe outside the Galaxy is considered. In [18] it is shown by a detailed model that a retardation force exist regardless if one assumes equation (3) or not.

3. Preliminary remarks

It is well known that Newtonian Gravity can be shown to be a limiting case of General Relativity (GR). To achieve this the following conditions are imposed:

- A weak field: $g_{\mu\nu} = \eta_{\mu\nu} + h_{\mu\nu}$, where g is the metric tensor, η flat Lorentz metric and h are small deviations from the flat metric ($|h_{\mu\nu}| \ll 1$).
- Non relativistic motion: $\tau \cong t$, $dx^0/d\tau \cong c$, $dx^i/d\tau = v^i \ll c$ where τ is the proper time, t coordinate time, x spatial coordinates, c the speed of light in vacuum, v speed of the object.
- $h_{00} = 2\phi/c^2$ where ϕ is the Newtonian potential.

As Newtonian Gravity has been used to explain celestial observations from its inception, primarily on the solar scale, and as GR showed Newtonian gravity can be considered a special case of GR in the weak field approximation, very little has changed when analyzing non-dense celestial objects observations such as, for example, galaxies; this is despite the fact these involve distances of many orders of magnitude beyond those for which Newtonian Gravity has been probed for experimentally.

In order to justify discrepancies between observed phenomena and Newtonian gravity, when light is used as a tracer for mass, a new type of matter dubbed Dark Matter (DM) has been added to the Newtonian model in the 1970s [7, 10, 11]. In order to comply with said observations and structure formation simulations a list of properties has been attributed to DM [7], which will not be listed here. However, to date, 50 years since its inception, DM has not been observed nor could any known particles be identified with its properties.

The similarities between General Relativity and Electromagnetic (EM) Theory have not gone unnoticed. While exact solutions have proven challenging due to the non-linear nature of the Einstein equations, within the weak field approximation, $h_{\mu\nu}$ can be approximated to its first order, making the equations linear, therefore superposable, yielding a Retarded Potential [3, 33] similar to that of EM theory [34].

Since the far field approach is not suitable within galaxies, or even at their edge, as the Galaxy is the source system, retardation theory [17–20, 22, 23, 42, 43] focus on the near field solutions, yielding a near field regime.

Trying to apply the potential of equation (4) to galactic rotation curves, we encounter an obstacle; we do not have an explicit expression for the density time-dependent function $\rho(\vec{x},\ t)$. However, we may assume that this function can be written as a combination of addition and multiplication of spatial and temporal functions:

$$\rho(\vec{x}',\ t) = n(\vec{x}') + m(t)n(\vec{x}') \tag{11}$$

which enables us [17], after some calculations, to write equation (4) as:

$$\phi_{ret} = -G\int\frac{\rho(\vec{x}',\ t)}{R}d^3x' - \frac{\ddot{M}}{M}\frac{G}{2c^2}\int R\rho(\vec{x}',\ t)d^3x' \tag{12}$$

where M is the total mass enclosed.

4. Methods

Here we provide a detailed methodology for calculating rotation curves and interpreting the mass flux to mass ratio. This work presents eleven rotation curves, for which the mid-plane circular velocity was derived from equation (12) by:

$$v(r) = \sqrt{\Upsilon\left(\frac{1}{r}\int\rho(\vec{x}')d^3x - \frac{r}{2c^2}\ddot{M}\right)}, \qquad R \simeq r \tag{13}$$

where Υ is the mass-to-light ratio (it is assumed that the contribution of the retardation correction is only significant outside the main mass of the Galaxy; for a more accurate treatment see [17]). Υ is deduced from the internal (Newtonian) part of the rotation curve. The spatial integral was calculated numerically using the hypergeometrical method [44] according to the mass model of the Galaxy; with the exception of one galaxy (NGC 3198) for which the thick disk model by Van der Kruit & Searle [45] was used (with scale height = scale length/4.8 [46]) to obtain a fit, galaxies were fitted using the double-thin mass model by Eckhardt and Pestaña [44]. The only free parameter after fixing the mass to light ration in the Newtonian regime is $\ddot{M}/M$, the relation of which to the depletion model (and also other quantities that may affect this parameter) are discussed below.

The data used to derive these rotation curves was taken from various literature sources [47–55]. The original data deprojection smoothing and processing of both the published observed photometry and the published observed rotation curves (RC) were adopted without further data processing attempts; as there are no free parameters when deriving gas velocities from the observed data, these too, when they exist, were adopted as is.

For comparison, the MONDian rotation curve for each galaxy was calculated in tandem, using the same parameters and the same mass-to-light ratio, however, unlike in various other works (for example [56]), a_0 was allowed to vary between galaxies as in its inception [26]; to date a physical justification for a universal a_0 does not exist, although a remarkable similarity of values emerges from fits to the data.

5. Results

Plots are presented in figure 1, figure 2 and summarized in table 1. For all plots the obtained change in mass flux (but not necessarily the mass flux) is negative, this means the flux of mass towards the center of the Galaxy decreases. As can be seen from the plots, for most cases the Newtonian component contribution is dominant in the initial rise of the curve. The mass-to-light ratio diverges but values are within reason and range from 0.6 (M33) to 9 for Galaxy 3917 which is a LSB galaxy. It can be seen that the RC calculated using Retardation Theory

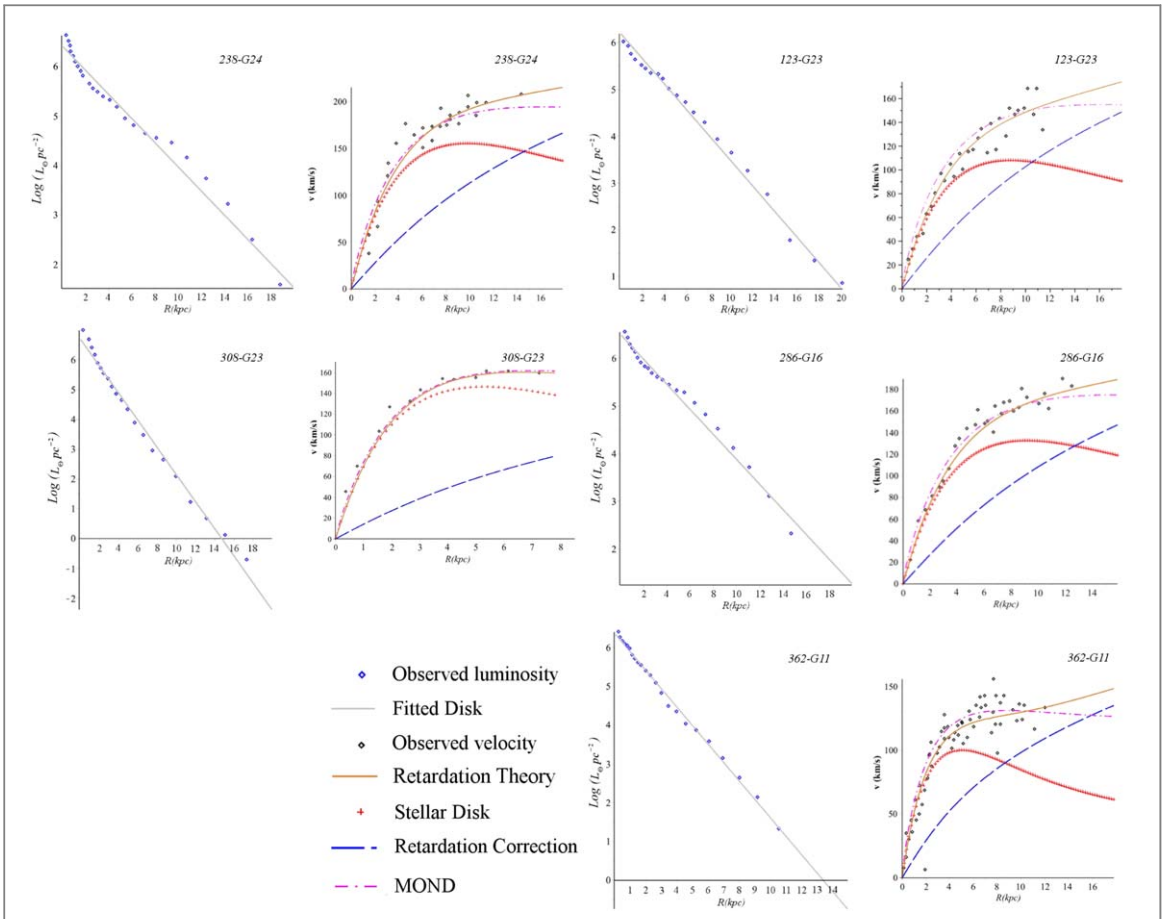

Figure 1. Fitted luminosity profiles and rotation curves. Panels show: observed luminosity (blue diamonds), exponential fits to the stellar disk (solid gray line), observed circular velocity (black diamonds), retardation theory fit (solid brown line), stellar Newtonian component (red crosses), retardation component (blue long dashes) and MONDian fit (magenta dash dot).

are able to match or improve the MONDian fit. Columns 6 & 7 of table 1 shows the values of the change in mass flux and birthrate index respectively. The data for the birthrate index was taken from Portinari *et al* [57] who averaged data from several sources, if data was not available for the specific galaxy type in Portinari et el. (e.g. type Sm; galaxy with a bulge) data was taken from Kennicut et. al [58]. A preliminary correlation between the mass flux change and the birthrate index can be seen, with similar values for similar galaxy types. While the value of $\ddot{M}/M$ suggests what seems to be quite a large decrease in flow towards the galactic center, the correlation with the birthrate index could explain this value as feedback from star formation processes has been shown to trigger mass outflows from the Galaxy via thermodynamical activity and induce pressure differences [59–61].

Data for galaxies 123-G23, 238-G24, 286-G16, 308-G23 and 362-G11 was taken from Persi and Salucci [48] and Mathewson, Ford, and Buchhorn [47]. In their paper Persi and Salucci divide the data into three different quality categories, data was taken from the category deemed by the researchers as of 'Excellent high quality rotation curves, suitable for individual detailed mass modelling'. The original RC data did not include error bars; as we are unfamiliar with observational weighted average methods nor with the galaxies' observed data we chose to present the data as in their paper. Luminosity data was fitted using the exponential disk profile and rotation curves were calculated accordingly, both are presented in figure 1. The mass-to-light ratios range from 0.75-1.3, which is in line with galaxy brightness. For type Sb (238-G24, 308-G23, 286-G16) the rate of change in the mass flux to mass ratio ranges between $-1.12 \cdot 10^{-24}$ to $-1.46 \cdot 10^{-24}$ and for type Sc (123-G23, 262-G11) it is $-2 \cdot 10^{-24}$ and $-3.2 \cdot 10^{-24}$ respectively. This correlates to the birthrate of 0.35 for type Sb and 0.9 for type Sc. The highest fitted mass-to-light ratio (M/L) in the sample is of 9 and is for Galaxy NGC 3197 which is a LSB, followed by NGC 3198 (M/L = 4.6) and NGC 300 (M/L = 2.5). While NGC 3198 has a small bulge, a good fit can be attained without it by subtracting the bulge data from the luminosity data, this results with brightness values similar to LSB galaxies. NGC 300 is a LSB galaxy. Therefore M/L values seem in line with the data, it is important to note that most RC fitted today use the DM paradigm which systematically underestimate the M/L ratios in order to avoid a 'doughnut' shape distribution of dark matter, therefore it is expected for our M/L ratio to differ from most current literature.

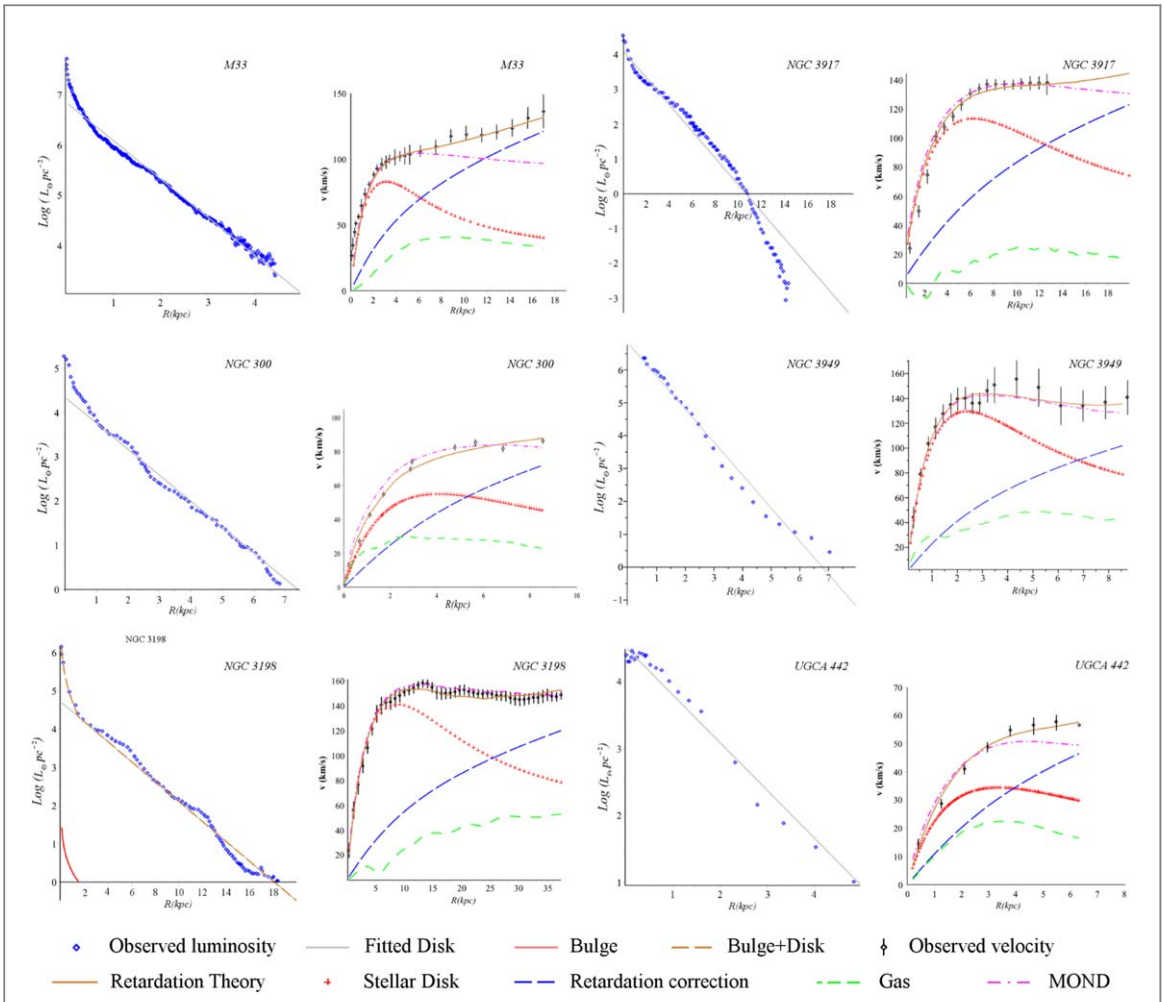

Figure 2. Fitted luminosity profiles and rotation curves. Panels show: observed luminosity (blue diamonds), exponential fits to the stellar disk (solid gray line), bulge fit (red solid line), sum of bulge + disk (long brown dashes), observed circular velocity (black diamonds w/error bar), retardation theory fit (solid brown line), stellar Newtonian component (red crosses), retardation force component (blue long dashes), gas component (short green dashes) and MONDian fit (magenta dash dot).

Table 1. Rotation Curve fitting data for 11 galaxies.

Galaxy Name (1)	Galaxy Type (2)	Mass Model (3)	Scale Length (pc) (4)	$\Sigma_0\,(M_\odot pc^{-2})$ (5)	$\ddot{M}/M$ $(10^{-24}/s^2)$ (6)	b (7)	M/L ratio $(M_\odot/L_\odot)$ (8)	a_0 (MOND) (m/s^2) (9)
NGC 3198[1]	Sbc	Thick	3848	110	−0.688	0.27*	4.6	$0.5 \cdot 10^{-10}$
238 G-24[2,3]	Sb	Double	4100	602	−1.12	0.35	0.9	$1.2 \cdot 10^{-10}$
308-G23[2,3]	Sb	Double	2198	812	−1.29	0.35	1.3	$1 \cdot 10^{-10}$
286-G16[2,3]	Sb	Double	3821	665	−1.46	0.35	0.75	$1.2 \cdot 10^{-10}$
N3917[4]	Scd	Double	2600	60	−1.5	0.69	9	$0.8 \cdot 10^{-10}$
123-G23[2,3]	Sc	Double	3675	493	−2	0.9	0.7	$1.2 \cdot 10^{-10}$
362-G11[2,3]	Sc	Double	2108	572	−3.2	0.9	0.9	$1.2 \cdot 10^{-10}$
N3949[5]	Sbc	Double	995	916	−4.8	0.9	2	$1.2 \cdot 10^{-10}$
M33[6,7]	Sc	Double	1315	944	−6.23	0.9	0.6	$0.8 \cdot 10^{-10}$
NGC 300[8]	Sc	Double	1700	354	−8.17	0.9	2.5	$0.7 \cdot 10^{-10}$
UGCA 442[9]	Sm	Double	1400	92	−14.6	1.67*	1	$0.25 \cdot 10^{-10}$

Columns are: (1) Name of the Galaxy. Observational data for each galaxy was taken from its respective reference (2) Galaxy type, (3) Mass model used for calculation where Double is short for double infinitesimally thin exponential disk model and Thick is short for exponential disk with a $sech^2$ distribution in the z-axis. (4) Exponential disk model scale-length given in parsecs, (5) Central mass density, (6) mass flux change-to-mass ratio, (7) star birthrate of the Galaxy type from Portinari *et al* [57] and Kennicutt *et al* [58]; data retrieved from Kennicutt *et al* is denoted with an asterisk*. (8) mass-to-light ratio (9) MOND acceleration constant. Sources: (1) [52]; (2) [48]; (3) [47]; (4) [50]; (5) [51]; (6) [53]; (7) [54]; (8) [55]; (9) [49].

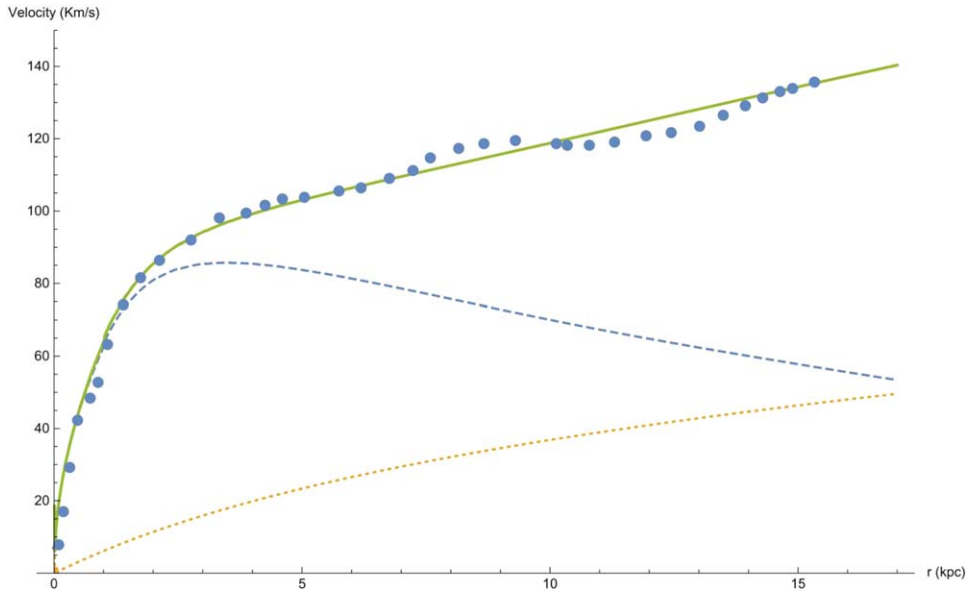

Figure 3. Rotation curve for M33. The observational points are taken from [53], the full line describe the complete rotation curve which is the sum of the dotted line describing the retardation contribution and the dashed line which is the Newtonian contribution.

The fit for galaxy NGC 3949 is not as good as others of our cases (although slightly better than MOND), as the rotation curve is not flat and exhibits a small 'wave' in its shape. Richards *et al* [51], similar to other literature, found that the rotation curve derived from the receding side of the HI velocity field rises faster than the approaching side, resulting in an asymmetric RC. It is possible that one side of the Galaxy is more active, or its surroundings has a larger mass reservoir and therefore the change in mass flux is inconsistent throughout and too local to attain a good fit with the homogeneous mass flux change we apply; Verheijen [50] notes a faint companion 1.5 arcmin to the north that may be interacting with this galaxy.

Galaxy UGCA 442 is a dwarf galaxy and its mass flux change is the highest in our sample; this result correlates well with the high star birthrate index for dwarf galaxies (1.67) as dwarf galaxies are characterized by star formation bursts and the star birthrate index relates to change in star formation rates.

The fit for galaxy M33 using retardation theory is significantly better than that of the MONDian curve. The change in mass flux is similar to other type Sc galaxies and its mass-to-light ratio is within reason (0.6) (this can be improved by using a more accurate estimation of the Newtonian and retardation contributions [17], which shows that the mass-to-light ratio in the Galaxy M33 is one with $|\ddot{M}| \simeq 9.12\ 10^{16}$ kg/s^2). The fitted rotation curve of M33 for a more accurate density profile is given in figure 3. To conclude this section and to expand on our recent publication [16] we shall present some additional results. Tomer Zimmerman & Roy Gomel have written there own fitting program for the retardation model, their quite convincing results are given in figure 4 for the Galaxy NGC247, and in figure 5 for the Galaxy NGC3917. Yuval Glass which is a student and research assistant of one of us (Professor Yahalom) has automated the fitting process, some of the impressive examples of his work (which include 143 galaxies of various types deserving a separate publication) is given below. Those include figure 6 for the Galaxy F568-V1, figure 7 for the Galaxy NGC1090, and figure 8 for the Galaxy NGC3521. Data for the above figures is obtained from the SPARC Galaxy collection [62].

6. Discussion

6.1. Origins of retardation

How can one reach an erroneous conclusion regarding the existence of 'dark matter'? By ignoring retardation effects and assuming that radial velocities are a result of some mysterious substance. We obtain for a spherically symmetric distribution [63]:

$$-\frac{v_c^2}{r}\hat{r} = \vec{F}_d = -\frac{GM_d(r)}{r^2}\hat{r} \tag{14}$$

where v_c is the speed of a particle of unchanging radius r and $M_d(r)$ is the dark matter within the radius r. Comparing equations (14) and (13), we deduce that the 'dark matter' mass can be calculated as follows:

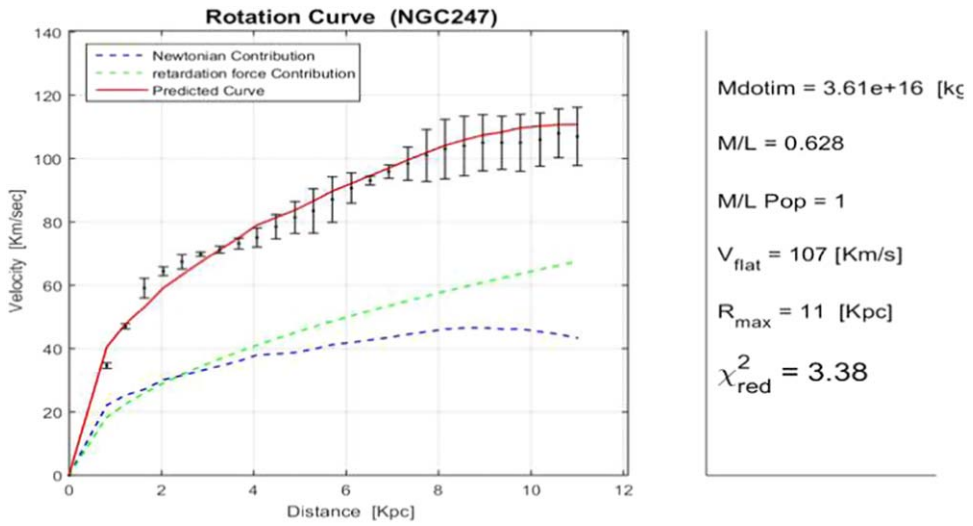

Figure 4. Rotation curve for NGC247 fitted to the retardation model, fitting parameters are given on the right hand side.

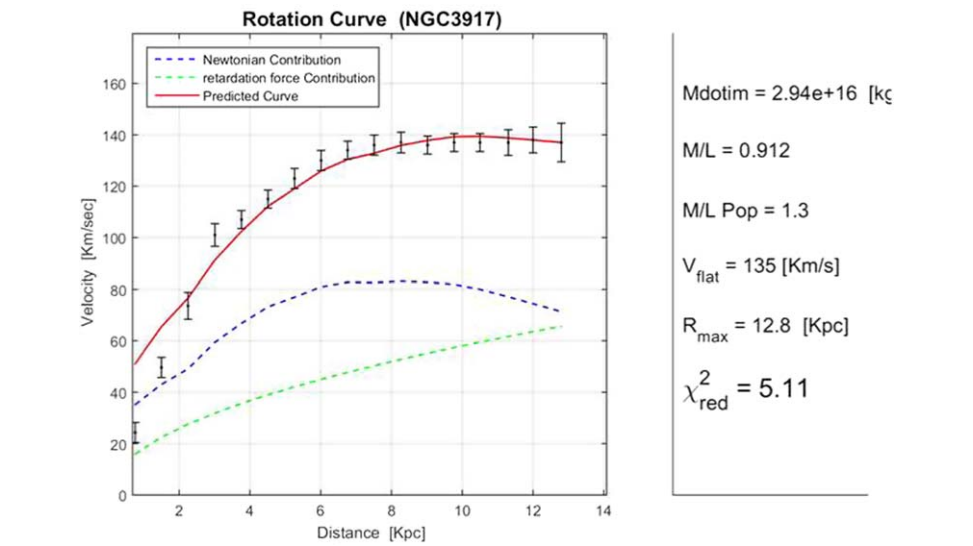

Figure 5. Rotation curve for NGC3917 fitted to the retardation model, fitting parameters are given on the right hand side.

$$M_d(r) = \frac{r^2|\ddot{M}|}{2c^2.} \tag{15}$$

Let us write the continuity equation:

$$\frac{\partial \rho}{\partial t} + \vec{\nabla} \cdot (\rho \vec{v}) = 0 \tag{16}$$

$\vec{\nabla}$ has its standard meaning in vector analysis. Let us now take a partial temporal derivative of equation (16) leading to:

$$\frac{\partial^2 \rho}{\partial t^2} + \vec{\nabla} \cdot \left(\frac{\partial \rho}{\partial t} \vec{v} + \rho \frac{\partial \vec{v}}{\partial t} \right) = 0. \tag{17}$$

Using equation (16) again we obtain the expression:

$$\frac{\partial^2 \rho}{\partial t^2} = \vec{\nabla} \cdot \left(\vec{\nabla} \cdot (\rho \vec{v}) \vec{v} - \rho \frac{\partial \vec{v}}{\partial t} \right). \tag{18}$$

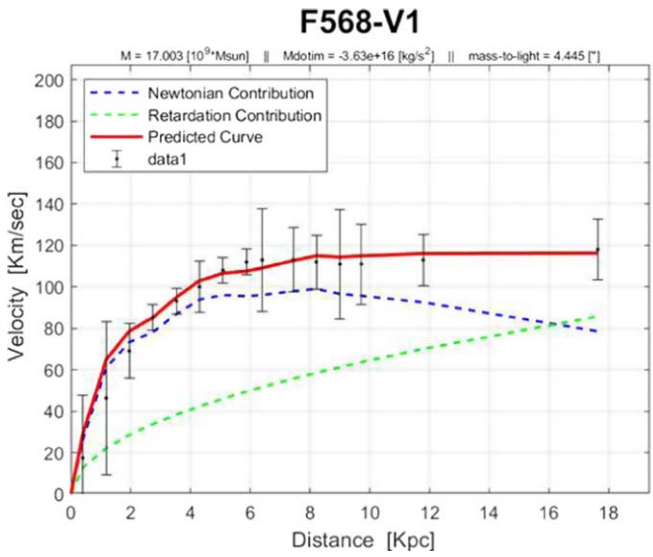

Figure 6. Rotation curve for F568-V1 fitted to the retardation model, fitting parameters are given above the plot.

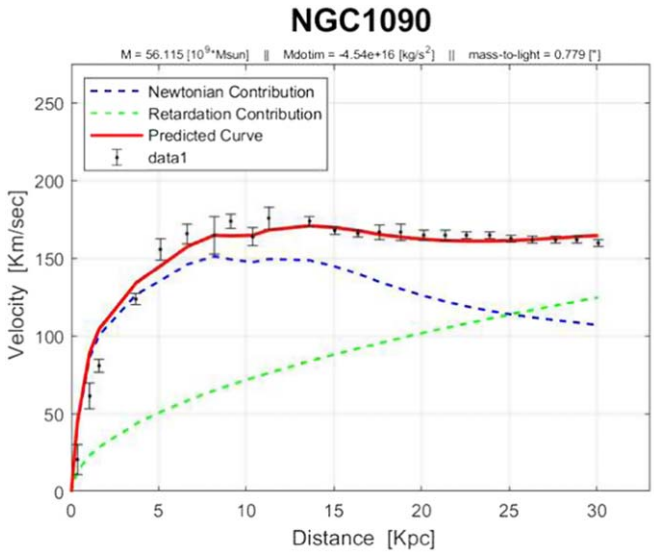

Figure 7. Rotation curve for NGC1090 fitted to the retardation model, fitting parameters are given above the plot.

We divide the left and right hand sides of the equation by c^2 and obtain:

$$\frac{1}{c^2}\frac{\partial^2\rho}{\partial t^2} = \vec{\nabla}\cdot\left(\frac{\vec{v}}{c}\left(\frac{\vec{v}}{c}\cdot\vec{\nabla}\rho + \rho\vec{\nabla}\cdot\left(\frac{\vec{v}}{c}\right)\right) - \rho\frac{1}{c}\frac{\partial\frac{\vec{v}}{c}}{\partial t}\right). \tag{19}$$

Since $\frac{\vec{v}}{c}$ is rather small in galaxies and galaxy clusters it follows that $\frac{1}{c^2}\frac{\partial^2\rho}{\partial t^2}$ is also small unless the density or the velocity have significant spatial derivatives. A significant acceleration $\frac{\partial\frac{\vec{v}}{c}}{\partial t}$ resulting from a considerable force can also have a decisive effect, this may be connected to star formation processes as discussed below. The depletion of available gas can also cause such gradients as we describe using a detailed model in [17]. Taking the volume integral of the left and right hand sides of equation (19) and using Gauss theorem we arrive at the following equation:

$$\frac{1}{c^2}\ddot{M} = \frac{1}{c^2}\int\frac{\partial^2\rho}{\partial t^2}d^3x = \oint d\vec{S}\cdot\left(\frac{\vec{v}}{c}\left(\frac{\vec{v}}{c}\cdot\vec{\nabla}\rho + \rho\vec{\nabla}\cdot\left(\frac{\vec{v}}{c}\right)\right) - \rho\frac{1}{c}\frac{\partial\frac{\vec{v}}{c}}{\partial t}\right). \tag{20}$$

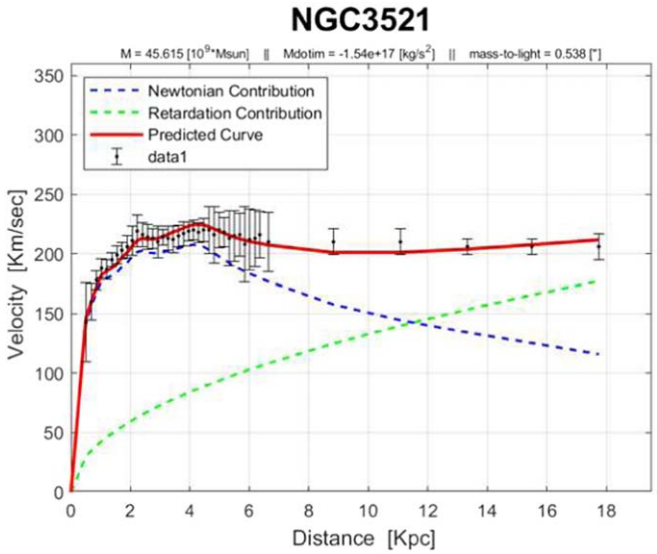

Figure 8. Rotation curve for NGC3521 fitted to the retardation model, fitting parameters are given above the plot.

The surface integral is taken over a surface encapsulating the Galaxy or galaxy cluster. This leads according to equation (15) to a 'dark matter' effect of the form:

$$M_d(r) = \frac{r^2}{2}\oint d\vec{S}\cdot\left(\frac{\vec{v}}{c}\left(\frac{\vec{v}}{c}\cdot\vec{\nabla}\rho+\rho\vec{\nabla}\cdot\left(\frac{\vec{v}}{c}\right)\right)-\rho\frac{1}{c}\frac{\partial\frac{\vec{v}}{c}}{\partial t}\right). \tag{21}$$

Thus we obtain the order of magnitude estimation:

$$\left[\frac{M_d(r)}{M}\right]\approx\left(\frac{v}{c}\right)^2\left[\frac{r}{l_\rho}+\frac{r}{l_v}+\frac{r}{l_d}\right] \tag{22}$$

In the above we define three gradient lengths:

$$l_\rho\equiv\frac{\rho}{|\vec{\nabla}\rho|},\qquad l_v\equiv\frac{v}{|\vec{\nabla}\cdot v|},\qquad l_d\equiv\frac{v^2}{|\partial_t v|} \tag{23}$$

We can also write:

$$\frac{1}{l_t}=\left[\frac{1}{l_\rho}+\frac{1}{l_v}+\frac{1}{l_d}\right] \tag{24}$$

in which the smallest gradient length will be the most significant one in terms of the 'dark matter' phenomena. Thus:

$$\frac{F_r}{F_N}=\left[\frac{M_d(r)}{M}\right]\approx\left(\frac{v}{c}\right)^2\left[\frac{r}{l_t}\right] \tag{25}$$

In the depletion model of [17] we assume that l_ρ associated with density gradients is the shortest length scale, this is only an assumption, other alternatives are possible as described below. For galaxies we have $\left(\frac{v}{c}\right)^2\approx 10^{-6}$, hence the factor $\frac{r}{l_t}$ should be around 10^6 to have a significant 'dark matter' effect.

6.2. The depletion model

In previous sections the free fitting parameter was the second derivative of the galactic mass, here we shall attempt to shed some light on its physical origin. It is intuitively obvious that as mass is accumulated in the Galaxy during its creation (a galaxy is formed by a fluctuation in the homogeneous primordial density that grows due to gravity) it must be depleted in the intergalactic medium. This is due to the fact that the total mass is conserved. Still it is of interest to see if this intuition is compatible with a model of gas dynamics, this will be studied here. For simplicity we assume that the gas as a barotropic ideal fluid and its dynamics is described by the Euler and continuity equations as follows:

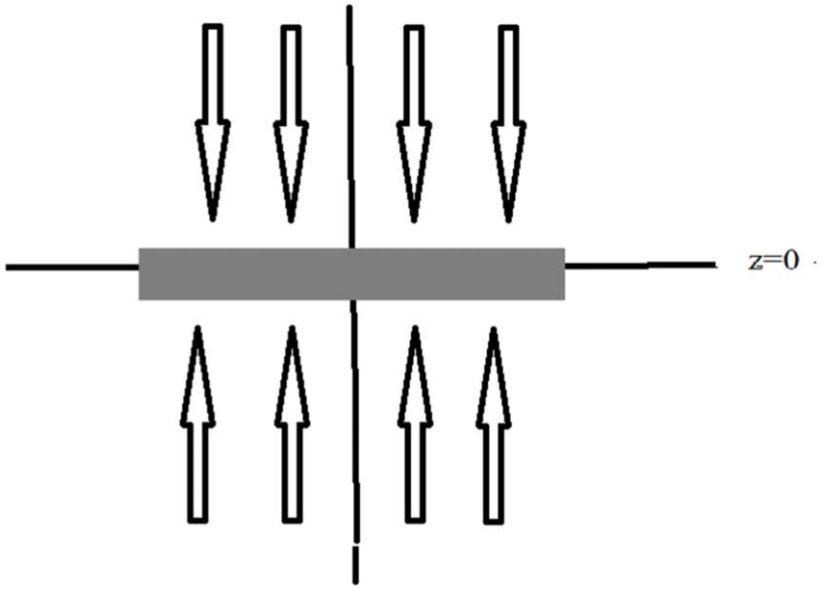

Figure 9. A schematic view of the galactic influx from a side view.

$$\frac{\partial \rho}{\partial t} + \vec{\nabla} \cdot (\rho \vec{v}) = 0 \tag{26}$$

$$\frac{d\vec{v}}{dt} \equiv \frac{\partial \vec{v}}{\partial t} + (\vec{v} \cdot \vec{\nabla})\vec{v} = -\frac{\vec{\nabla} p(\rho)}{\rho} - \vec{\nabla}\phi \tag{27}$$

In which the pressure $p(\rho)$ is assumed to be a given function of the density, $\frac{\partial}{\partial t}$ is a partial temporal derivative and $\frac{d}{dt}$ is the material temporal derivative. We have neglected viscosity terms due to the gas low density. For simplicity we assume axial symmetry, hence all variables are independent of the azimuthal angle θ. Moreover, the mass influx coming from above and below the Galaxy is much more significant as compared to the influx coming from the galactic edge. This is due to the large difference of the Galaxy surfaces perpendicular to the z axis compared to the area of its edge. In such circumstances the edge mass influx is less important and we can assume a velocity field of the form:

$$\vec{v} = v_z(\bar{r}, z, t)\hat{z} + v_\theta(\bar{r}, z, t)\hat{\theta}. \tag{28}$$

$\hat{z}$ and $\hat{\theta}$ are unit vectors in the z and θ directions respectively. $\bar{r}$ is a radial cylindrical coordinate. The influx is described schematically in figure 9.

In this case the continuity equation (16) will take the form:

$$\frac{\partial \rho}{\partial t} + \frac{\partial (\rho v_z)}{\partial z} = 0 \tag{29}$$

Defining the quantity:

$$\gamma \equiv \rho v_z \Rightarrow \rho = \frac{\gamma}{v_z} \tag{30}$$

and using the above definition equation (29) takes the form:

$$\frac{\partial (\frac{\gamma}{v_z})}{\partial t} + \frac{\partial \gamma}{\partial z} = 0 \tag{31}$$

Assuming for simplicity that v_z is stationary and defining the auxiliary variable t_z:

$$t_z \equiv \int \frac{dz}{v_z} \tag{32}$$

we arrive at the equations:

$$\frac{\partial \gamma}{\partial t} + \frac{\partial \gamma}{\partial t_z} = 0. \tag{33}$$

This equation can be solved easily as follows:

$$\gamma(\bar{r}, z, t) = f(t - t_z), \qquad f(-t_z) = \gamma(\bar{r}, z, 0) = v_z \rho(\bar{r}, z, 0) \tag{34}$$

for the function $f(x)$ which is fixed by the density initial conditions and the velocity profile.

Let us now turn our attention to the Euler equation (27), for stationary flows it takes the form:

$$(\vec{v} \cdot \vec{\nabla})\vec{v} = -\frac{\vec{\nabla} p(\rho)}{\rho} - \vec{\nabla}\phi \tag{35}$$

According to equation (28):

$$\vec{v} \cdot \vec{\nabla} = v_z \frac{\partial}{\partial z} + \frac{v_\theta}{\bar{r}} \frac{\partial}{\partial \theta} \tag{36}$$

Now writing equation (35) in terms of its components we arrive at the following equations:

$$v_z \frac{\partial v_z}{\partial z} = -\frac{1}{\rho} \frac{\partial p}{\partial z} - \frac{\partial \phi}{\partial z} \tag{37}$$

$$-\frac{v_\theta^2}{\bar{r}} = -\frac{1}{\rho} \frac{\partial p}{\partial \bar{r}} - \frac{\partial \phi}{\partial \bar{r}}, \qquad \left(\frac{\partial \hat{\theta}}{\partial \theta} = -\hat{\bar{r}}\right). \tag{38}$$

It is usually assumed that the radial pressure gradients are negligible with respect to the gravitational forces and thus we arrive at the equation:

$$\frac{v_\theta^2}{\bar{r}} \simeq \frac{\partial \phi}{\partial \bar{r}}, \tag{39}$$

As for the z-component part of the Euler equation (35) it can be easily written in terms of the specific enthalpy $w(\rho) = \int \frac{dP}{\rho}$ in the form:

$$\frac{\partial}{\partial z}\left(\frac{1}{2} v_z^2 + w(\rho) + \phi\right) = 0 \Rightarrow \frac{1}{2} v_z^2 + w(\rho) + \phi = C(r, t). \tag{40}$$

We recall that ρ depends on v_z through equations (30) and (34):

$$\rho(\bar{r}, z, t) = \frac{\gamma}{v_z} = \frac{f\left(t - \int \frac{dz}{v_z}\right)}{v_z} \tag{41}$$

As both the specific enthalpy and the gravitational potential are dependent on the density, equation (40) turns into a rather complicated nonlinear integral equation for v_z. However, many galaxies are flattened structures, hence it can thus be assumed that the pressure z gradients are significant as one approaches the galactic plane. We will thus assume for the sake of simplicity that the pressure gradients balance the gravitational pull of the Galaxy and thus v_z is just a function of r in which case the convective derivative of v_z vanishes. The above assumption holds below and above the galactic plane but not at the galactic plane itself. This suggests the following simple model for the velocity v_z (see figure 9):

$$v_z = \begin{cases} -|v_z| & z > 0 \\ |v_z| & z < 0 \end{cases} \tag{42}$$

in which $|v_z|$ is a known function of $\bar{r}$. The velocity field is discontinuous at the galactic plane due to our simplification assumptions, but of course need not be so in reality. We also assume for simplicity that the velocity field $|v_z|$ is constant for $\bar{r} < r_m$ and vanishes for $\bar{r} > r_m$. According to equation (34) the time dependent density profile is fixed by the density initial conditions. In this section we will deal with the density profile outside the galactic plane. We consider an initial density profile as follows:

$$\rho_o(\bar{r}, z, 0) = re(z)[\rho_1(\bar{r}) + \rho_2(\bar{r}) e^{k|z|}],$$
$$re(z) = \begin{cases} 1 & |z| < z_i \\ 0 & |z| \geqslant z_i \end{cases} \tag{43}$$

in which the rectangular function $re(z)$ keeps the exponential function from diverging. The density profile is depicted in figure 10. We assume that ρ_2 is negative and thus the density becomes dilute at distances far from the galactic plane. As v_z is constant both above and below the galactic plane, $t_z = \frac{z}{v_z}$ up to a constant. And now it is easy to deduce from equation (34) the functional form of $f(\beta)$ ($\beta = -t_z$):

$$f(\beta) = v_z re(-v_z \beta)[\rho_1 + \rho_2 e^{k|v_z \beta|}] \tag{44}$$

And hence according to equation (41) the time dependent density function for matter outside the galactic plane is obtained:

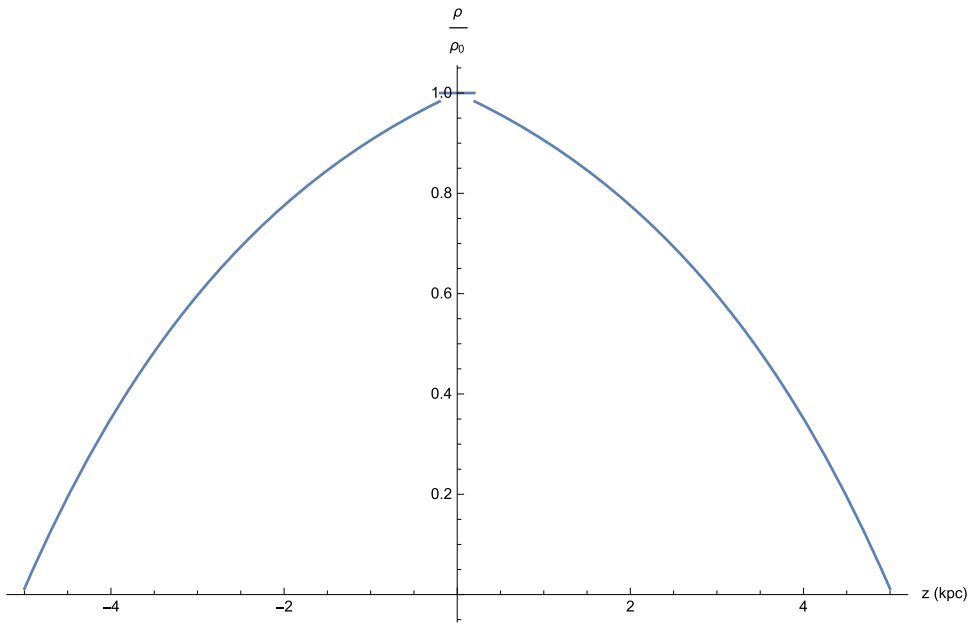

Figure 10. An initial density profile out side the galactic plane. In which $\rho_0 = \rho_1 + \rho_2$, $\frac{\rho_2}{\rho_1} = -0.2$ and $z_i = 5$ (kpc) and $k = 0.32$ (kpc^{-1}).

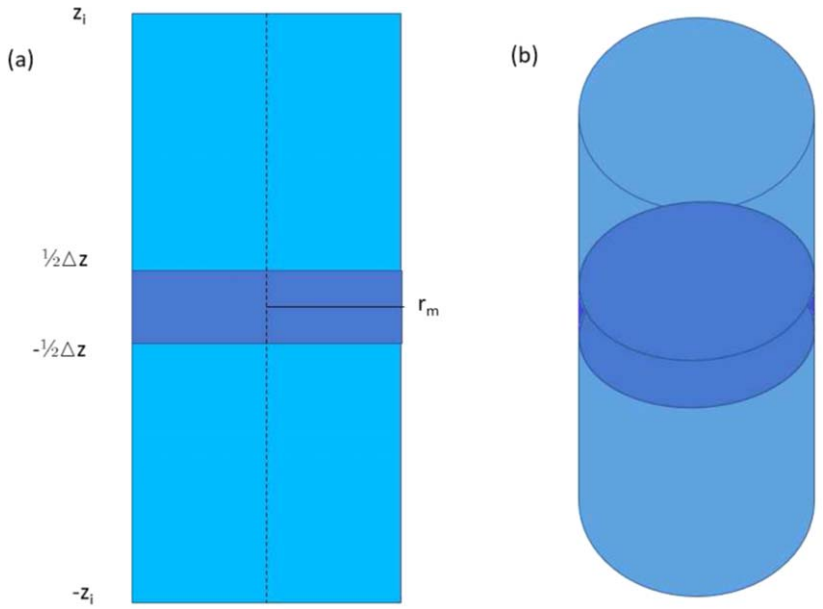

Figure 11. The mass column defined by the Galaxy (a) Side view (b) Three dimensional view.

$$\rho_o(\bar{r}, z, t) = \frac{\gamma}{v_z} = re(z - v_z t)[\rho_1(\bar{r}) + \rho_2(\bar{r})e^{k|z - v_z t|}] \tag{45}$$

The density of matter outside the galactic plane will vanish for $t > t_m = \frac{z_i}{|v_z|}$, hence we will discuss only the duration of $t < t_m$. Let us look at the mass contained in the cylinder defined by the Galaxy (see figure 11) and let us assume that the total mass in that cylinder is M_T. Now the mass outside the galactic disk will be:

$$M_o(t) = 2\pi\left[\int_{-z_i}^{-\frac{1}{2}\Delta z} dz \int_0^{r_m} d\bar{r}\bar{r}\rho_o(\bar{r}, z, t) + \int_{\frac{1}{2}\Delta z}^{z_i} dz \int_0^{r_m} d\bar{r}\bar{r}\rho_o(\bar{r}, z, t)\right] \tag{46}$$

Hence the mass in the galactic disk is:

$$M(t) = M_T - M_o(t) \tag{47}$$

And the galactic mass derivatives are:

$$\dot{M}(t) = -\dot{M}_o(t), \qquad \ddot{M}(t) = -\ddot{M}_o(t) \tag{48}$$

Inserting equations (45) into (46) we may calculate $M_o(t)$:

$$M_o(t) = 2\left[\lambda_1\left(z_i - |v_z|t - \frac{1}{2}\Delta z\right) + \frac{\lambda_2}{k}(e^{kz_i} - e^{k(|v_z|t+\frac{1}{2}\Delta z)})\right] \tag{49}$$

in which:

$$\lambda_1 \equiv 2\pi\int_0^{r_m} d\bar{r}\bar{r}\rho_1(\bar{r}), \qquad \lambda_2 \equiv 2\pi\int_0^{r_m} d\bar{r}\bar{r}\rho_2(\bar{r}). \tag{50}$$

Now calculating the second derivative of $M_o(t)$ and using equation (48) leads to the result:

$$\ddot{M}(t) = -\ddot{M}_o(t) = 2k|v_z|^2 e^{\frac{1}{2}\Delta zk}\lambda_2 e^{k|v_z|t}. \tag{51}$$

We shall denote:

$$\alpha \equiv k|v_z|, \qquad \tau \equiv \frac{1}{\alpha}, \qquad \ddot{M}(0) = 2k|v_z|^2 e^{\frac{1}{2}\Delta zk}\lambda_2. \tag{52}$$

Thus:

$$\ddot{M}(t) = \ddot{M}(0)e^{\frac{t}{\tau}}. \tag{53}$$

So even if $\ddot{M}(0)$ is small, $\ddot{M}(t)$ will soon become exponentially large at a time scale depending on τ which in turn depends on the density gradient (see previous subsection) and the velocity of the falling gas (which can be quite small). Of course the above depletion model is highly simplified and other effects such as galactic winds may well play a rule as discussed in the next section.

6.3. Correlation with star birthrate index

We have presented here a sample of galaxies for which retardation theory was able to reproduce rotation curves in good agreement with observational data, fitting different types of galaxies, with different rotation curve shapes. In the fitting process two parameters were used as free fitting parameters, the mass-to-light ratio, for which values are within reason, and the change in mass flux which is part of the retardation effect coefficient of equation (13) (second term). As this coefficient is a function of the mass flux, the retarded effect contribution can be fine-tuned for each galaxy, resulting in a versatility which enables us to produce various RC shapes, from the prevalent flat rotation curve (308-G23, for example) to M33's rising curve. The change in the mass flux to mass ratio was considered cohesive throughout the Galaxy, this is in line with a radial mass flow, or, mass flux towards the galactic center which varies with time. Radial or non-circular mass flows between the Interstellar Medium (ISM) and the Intergalactic Medium (IGM) have been recorded by various works since the 1960's [64–66]. Although this parameter was fitted for each galaxy separately, a trend in its values is seen; a preliminary correlation between the change in mass flux towards the center of the Galaxy and the Galaxy's star birthrate index, estimated by galaxy type, was observed.

Star formation feedback has been shown to generate mass outflow via superwinds, large-scale galactic outflows [64]. Woo *et al* [61] saw that the correlation between star formation rate (SFR) and ionized gas outflow is clear, while other works [59, 60, 67–70] show the velocity of these winds to be very large, and can exceed the Galaxy's escape velocity. This clear correlation between SFR and mass outflows suggest that a change in the star formation rate would be expressed as a change in said mass outflow. The star birthrate index is defined by [58]:

$$b = \frac{SFR}{\langle SFR \rangle_{past}} \tag{54}$$

which relates to change in SFR. Therefore, the correlation between star birthrate index and the change in mass flux towards the galactic center may be linked via the change in mass outflows.

6.4. Truncation of the Taylor series

As the contribution of the second term of equation (13) is large, we must justify the assumption we made yielding equation (7), namely, neglecting terms of order $n > 2$ of equation (4). While one could assume depletion of Intergalactic Medium (IGM) with an exponential decay, in which case terms of order $\mathcal{O}(R/c)^3$ and higher might be shown to be neglected [18], the correlation with the birthrate index suggests that the contribution to the change in mass flux due to SFR activity to the $\ddot{M}/M$ coefficient is significant. Therefore, we delve into the processes which lead to galactic superwinds. While the field is relatively young and the mechanism is not fully understood, various observations and simulations shed light on a possible mechanism [60, 64, 68, 71]: Galactic superwinds are powered by the energy deposited in the interstellar medium by massive stars via supernovae (SNe) and stellar winds. The ejecta from hot stars and SNe in the star burst region quickly interact and mix with the surrounding gas to produce a cavity of hot material, this over-pressurized 'bubbles' of hot material propagate and expand in the least resistance path, propagating laterally in the plane of the Galaxy and carried vertically out of the disk. As this bubble expands it carries cold gas and dust along with it, after which it will evolve into a 'blowout' phase as it accelerates outwards and fragments, propagating out into the IGM. As mentioned, the trigger mechanism of these super winds is SNe and solar winds activity, these are highly localized (∼1 kpc) and relatively instantaneous when compared to galactic superwinds which have been observed at great distances from galaxies enriching the IGM with metals over 100 kpc away [72], with outflows spanning from 0.1 to 10Myr [64]. As $\ddot{M}/M$ is taken to be cohesive throughout the Galaxy, the change in mass flux would correlate with that of superwinds while the trigger processes are too small or too short to have a detectable effect on midplane mass flux towards the galactic center. Of high interest to this argument is Heckman *et al*'s [68] work, in which they observe that for a typical outflow matter is injected at roughly zero velocity, therefore gas is 'loaded' into the outflow at $v \approx v_{sys}$ [6] and is accelerated up to some v_{term} which is significantly larger than v_{sys} (x4 for the largest value in their sample). As mass is loaded at 'zero' and then accelerated outwards we believe it is reasonable to assume that while the mass outward acceleration in superwinds disrupt the midplane mass flux towards the galactic center, higher derivatives contribution effects which would have disrupted this pre-loaded mass are negligible in this phenomenon.

6.5. The size of the second term coefficient

The values we get for the free fitting parameter $\ddot{M}/M$ range between $-0.688 \cdot 10^{-24} s^{-2}$ to $-14.6 \cdot 10^{-24} s^{-2}$. While direct measurement of interstellar material are hard due to dust and kinematics, estimations for Galactic outflows, Galactic winds and starburst superwinds range from tens to over a thousand Solar masses per year [59]. If one assumes a galactic mass of 10 billion solar masses, this estimation would yield a ratio of mass flux to mass range of $3.17 \cdot 10^{-17}$ to $3.17 \cdot 10^{-15}$ per second (or $\dot{M}/M$). However, said outflow mass flux estimations are based on a constant average mass flow over the wind's lifetime while the observational picture does not suggest constant mass flux within the galactic disk. Mass outflows have been observed to be correlated with SFR activity; Rupke *et al* [69], for example, received a linear relation between mass outflows and SFR which is larger than one ($dM/dt/SFR > 1$) while Martin [60] found that for dwarf galaxies this relation may be a few times the rate of SFR. This correlation between outflows and SFR activity means that a change in the SFR activity will be expressed as a matching or greater, change in mass outflow. More over, as detailed in the previous section, galactic super winds are driven by stellar winds and supernovae, generating blast waves [73, 74], and as Heckman *et al* [68] and others (for example [60, 70, 75]) observed, the velocities of mass loaded into the super wind can be times larger than the systematic rotational velocity, it is estimated that between $10^5 - 10^8 M_\odot$ of ionized gas takes part in galactic super winds outflows [64, 68]. While direct measurements and observations of the activity in the ISM are proven very difficult due to dust, remnants and kinematics, one observation which strengthen large quantities of mass leaving the galaxies is the 'missing metals problem' [76]. The ISM contains, among others, heavier than hydrogen components such as He, C, N, O, Ne, Fe and Dust (Helium, which is estimated to make up8% of the ISM by number, contributes 40% by mass) [77]. While metals are formed exclusively in the hot cores of stars, their amounts in galaxies fall well short of the amount expected to be produced by their stars; it is estimated that galaxies retain only 20%–50% of their metals while the IGM is enriched with metals to a detectable level estimated of 0.3 solar metalicity [66, 68, 76]; superwinds are thought to be the main mechanism for this enrichment, therefore carrying metals as well. Given the large mass quantities which reside in the ISM, the strong acceleration within galactic superwinds, galactic superwinds mechanism of shells removing material from the

[6] v_{sys} denotes the systematic rotational velocity, the velocity observed at the 'plateau' of the galactic rotation curve.

disk which only in part leaves the Galaxy, and estimation of mass carried out of the Galaxy of $10^5 - 10^8 M_\odot$ for gas alone, it seems that our change in the galactic midplane mass flux to mass ratio towards the galactic center range of $-0.688 \cdot 10^{-24} s^{-2}$ to $-14.6 \cdot 10^{-24} s^{-2}$ (or $\ddot{M}/M$) is within reason, though, of course, more research is needed to shed light on mechanism and quantities.

If mass were to leave the Galaxy at such constant rate throughout the Galaxy's life it would, of course, deplete the Galaxy's entire mass making it unstable. However, its correlation with birthrate index suggests this term is not static but changes in tandem with galactic SFR processes. Galactic superwinds can span from 0.1 to 10 Myr [64] therefore the size of $\ddot{M}/M$ is only static in the context of said observational time and is not static for the lifetime of the Galaxy, nor for the lifetime of the galactic super wind (more details about correct and erroneous estimation of galactic mass, based on calculated second derivatives can be found in [17]).

6.6. Dwarf galaxies

Unlike most spiral galaxies, the rotation curve shape of dwarf galaxies usually does not conform to the flat rotation curve (see, for example, Swaters *et. al* [78] or Haghighi and Rahvar [79]) and its shape can differ from it greatly. While our sample contains only one Dwarf galaxy, the observed star formation bursts in dwarf galaxies could suggest that the retarded effect is much stronger in dwarf galaxies than in spiral galaxies; this may explain this deviation from the flat rotation curve. In addition, localized strong activity could account for non-smooth 'wiggly' curves observed in some dwarf galaxies. We therefore believe that in order to further study the galactic rotation curves of dwarf galaxies, a more detailed approach, one which investigates the individual galaxy's dynamics and kinematics in tandem with the observed rotation curve should be taken; however, such research is currently beyond our scope.

The correlation with the birthrate index is an encouraging result which strengthens the theory underlying assumptions of effects due to changes in mass flux. The values used here for the galactic star birthrate index were not individually matched per galaxy but provided by works [57, 58] which try to estimate the star birthrate index, which relates to the change in SFR, by galaxy type. We therefore believe that further refining these values, investigating the mechanism and correlation between the change in mass flux and the change in SFR per galaxy may produce an additional tool for investigating galactic dynamics and kinematics, by using the relatively simple to observe rotation curve.

It is important to note, however, that the value we receive for our change in the mass flux to mass ratio coefficient is deduced by fitting and gives the net change in mass flux to mass ratio needed in order to receive good rotation curve fits. While the large mass quantities carried by galactic superwinds and their kinematics seem to be able to account for this value, more research is needed in order to elucidate the mechanism and determine accurate quantities and their exact contribution, which may differ from the required net change. Gas accretion, for example, currently estimated at $0.1 - 0.25 M_\odot yr^{-1}$ or even ten times as that [65], may reduce mass flux towards the galactic center by slowing down due to changing thermal and pressure differences between the ISM and IGM or due to HI depletion of the IGM. Other dynamical processes and forces may be at play as well.

6.7. Relation to MOND

Before we conclude the discussion section we would like to briefly discuss the relations between retarded gravity and modified Newtonian dynamics (MOND) [30]. MOND suggests corrections to Newtonian gravity when acceleration is small, further more it suggests an interpolation function connecting the high and low acceleration regimes. Those aspects are analyzed below.

6.7.1. The low acceleration regime

MOND is a theory which suggests an amendment to Newton's gravity when the acceleration a is smaller than $a_0 (\simeq 1.2 \cdot 10^{-10}\ \mathrm{m/s^2})$, it is exacly the same as Newton's gravity for $a \gg a_0$. Retarded gravity is significant according to equation (25) if the following inequality is satisfied:

$$\frac{v^2}{c^2}\frac{r}{l_t} > fr \tag{55}$$

Where $fr \equiv \frac{F_r}{F_N}$ is a given fraction of the Newtonian gravity, say 1%. Let us now investigate the acceleration expression: $a = \frac{v^2}{r}$. It follows that if the finite velocity of the gravitational field is of importance:

$$a = \frac{v^2}{r} > a_c(r) \equiv fr\frac{c^2 l_t}{r^2} \tag{56}$$

Now, $a_c(r)$ is proportional to $\frac{1}{r^2}$ this means that this inequality will be satisfied eventually for large enough r. It follows that 'missing mass' manifestations can be analyzed in terms of acceleration as is suggested by the MOND theory. Notice that acceleration is not small with respect to a universal constant a_0 in order to facilitate what one may consider as a 'dark matter' manifestation. Rather, acceleration in the absolute sense must be larger than the

critical quantity $a_c(r)$. However, the inequality becomes easier to satisfy at large distances, for which the acceleration is minute. A dimunitive acceleration is of course the hallmark of MOND and specifies the values for which MOND corrections are indeed required.

6.7.2. Interpolation formula

MOND [26] declares that the force of gravity should modified as follows:

$$\vec{F}_M = -\frac{GM}{\mu(\frac{a}{a_0})r^2}\hat{r} \tag{57}$$

μ designates the interpolation function that should have a unity value if $a_0 \ll a$. Here we assume a novel type of interpolation function[7]:

$$\mu(x) = \frac{x^2}{\sqrt{1+x^4}} = \frac{1}{\sqrt{1+x^{-4}}} \quad \Rightarrow \quad \mu(\frac{a}{a_0}) = \frac{1}{\sqrt{1+\left(\frac{a_0}{a}\right)^4}}. \tag{59}$$

Provided that $a \ll a_0$, $\mu \simeq \left(\frac{a}{a_0}\right)^2$. Consider a particle revolving in a constant radius, it will thus be subject to a centrifugal acceleration of $a = \frac{v^2}{r}$ and we will have a MONDian force of the type:

$$\vec{F}_M = -\frac{GMa_0^2}{v^4}\hat{r} \tag{60}$$

Provided that v is constant at a distance far away which also coincides with the 'deep' MOND regime, this formula resembles the retardation force contribution of equation (8) and thus we obtain a formula for the mass second derivative:

$$|\ddot{M}| = \frac{2Ma_0^2c^2}{v^4}. \tag{61}$$

Leading to the Tully-Fisher equation:

$$M = kv^4, \qquad k = \frac{|\ddot{M}|}{2a_0^2c^2} \tag{62}$$

alternatively we may write a_0 as a function of $|\ddot{M}|$ in the following form:

$$a_0 = \frac{v^2}{c}\sqrt{\frac{|\ddot{M}|}{2M}}. \tag{63}$$

From this point of view retarded gravity if of MONDian form but with a novel interpolation expression:

$$\vec{F}_M = -\frac{GM}{\mu(\frac{a}{a_0})r^2}\hat{r} \simeq \vec{F}_N + \vec{F}_{ar} \tag{64}$$

7. Retardation theory and quantum field theory

Before we conclude, we shall discuss briefly the possibility that quantum field theory effects are related to galactic rotation curves and also in what sense is retardation theory a field theory. We notice the following:

1. Most scientific & technological disciplines do not use quantum field theory (QFT), those include all engineering disciplines (civil, mechanical, and electronic engineering). But also disciplines that are involved with exceedingly small scales such as material science, solid state physics, molecular physics, and atomic physics (scales of about 10^{-10} meters).
2. Moreover, even nuclear physicists rarely use QFT (scales of about 10^{-15} meters).
3. The only scientific discipline in which QFT is the main tool is elementary particle physics.

[7] A standard interpolation function is for example:

$$\mu(x) = \frac{x}{\sqrt{1+x^2}} \quad \Rightarrow \quad \mu\left(\frac{a}{a_0}\right) = \frac{1}{\sqrt{1+\left(\frac{a_0}{a}\right)^2}}. \tag{58}$$

4. It is generally accepted that if the electric field does not surpass the Schwinger limit: $\sim 10^{18}$ V/m, or the magnetic field is well below $\sim 4\ 10^{9}$ T, QED (QFT of electromagnetic fields) can be safely ignored as we do in the current work. Having said that we notice, however, that QED also works at low energy. A small shift of the hydrogen energy levels (Lamb's shift) is not described by classical electrodynamics only by QED. Moreover, spontaneous emission is believed to be described by QED and not classical electrodynamics.
5. In the current work it is shown that (classical) gravitational forces will suffice to describe galactic rotational curves. Hence, we do not need to consider any other field even in a weak classical form and certainly not its high field QFT effects.
6. The physics of the solar system can be described to a very accurate level without the use of QFT, planet trajectories are described to high accuracy by simply using Newtonian gravity. More refined effects in the solar system such as the anomalous precession of Mercury's perihelion are explained by general relativity without the need to use QFT.
7. The galactic system is many orders of magnitude larger than the solar system, hence there is not even the slightest chance that QFT will be relevant (given that even molecular physics can be explained without it).

Finally, we notice that both the equations of weak field general relativity (which is retarded gravity) and QFT satisfy Lorentz symmetry. In this sense one can think of retarded gravity as a field theory on a flat Lorentzian background.

8. Conclusion

It is interesting to note the similarity between Retardation Theory's potential with that of Mannheim's Conformal Gravity early linear potential [27, 28], a theory which seeks to replace GR and has been very successful reproducing rotation curves:

$$\phi^*(r) = -\frac{\beta^* c^2}{r} + \frac{\gamma^* c^2}{2} r \tag{65}$$

where $\phi^*(r)$ is the potential per unit solar mass and $\beta^* = GM_\odot/c^2$, to that of equation (4). If one were to equate this with equation (4) then γ^* would equal $\gamma^* = -G\ddot{M}/c^4$.

While other theories and paradigms seek to modify or replace current existing theories, Retardation Theory does not strive to change General Relativity nor the Newtonian limit of GR when it is appropriate. The theory seems elegant, with only two free parameters whose origin is clear, with good results reproducing RC for our sample (and indeed for a much large sample) and preliminary correlation of change in mass flux with star birthrate index (which relates to the change in SFR and therefore mass outflows), indicating the effect of mass outflow on rotation curves may be significant. We believe the theory has great potential for future research and are currently studying additional aspects of the theory. We also mention that using the weak gravitational field we have also obtained recently an improvement regarding the estimation of Mercury's perihelion precession [31, 32] but this is on a completely different scale.

Acknowledgments

One of us (MW) would like to thank A. Kashi and A. M. Michaelis for useful conversations. Two of us (MW and AY) would like congratulate our senior collaborator Professor Lawrence Paul Horwitz for his ninety two birthday. Also we would like to thank Tomer Zimmerman, Roy Gomel & Yuval Glass for sharing with us their results.

Data availability statement

No new data were created in this study.

ORCID iDs

Michal Wagman https://orcid.org/0000-0001-6755-9405
Lawrence Paul Horwitz https://orcid.org/0000-0003-4109-1896
Asher Yahalom https://orcid.org/0000-0001-6679-3320

References

[1] Einstein A 1916 Näherungsweise integration der feldgleichungen der gravitation *Sitzungsberichte der Königlich Preussischen Akademie der Wissenschaften Berlin* Part 1 (The Prusssian Academy of Sciences) pp 688–96
[2] Eddington A S 1923 *The Mathematical Theory of Relativity* (Cambridge University Press)
[3] Weinberg S 1972 *Gravitation and Cosmology: Principles and Applications of the General Theory of Relativity* (Wiley)
[4] Misner C W, Thorne K S and Wheeler J A 1973 *Gravitation* (W.H. Freeman & Company)
[5] Narlikar J V 1993 *Introduction to Cosmology* IInd edn (Cambridge University Press)
[6] Zwicky F 1937 On a new cluster of nebulae in pisces *Proc. Natl. Acad. Sci. U S A.* **23** 251–6
[7] de Swart J G, Bertone G and van Dongen J 2017 How dark matter came to matter *Nature Astronomy* **1** 0059
[8] Yahalom A 2023 The virial theorem for retarded gravity *International Journal of Modern Physics D* (Honourable Mention Gravity Research Foundation)
[9] Volders L M J S 1959 Neutral Hydrogen in M33 and M101 *Bull. Astr. Inst. Netherl.* **14** 323
Rubin V C, Ford W K Jr, Thonnard N and Roberts M S 1976 Motion of the galaxy and the local group determined from the velocity anisotropy of distant Sc I galaxies. I. the data and II. the analysis for the motion *Astrophys. J.* **81** 719–37
[10] Rubin V C and Ford W K Jr 1970 Rotation of the andromeda nebula from a spectroscopic survey of emission regions *Astrophys. J.* **159** 379
[11] Rubin V C, Ford W K Jr. and Thonnard N 1980 Rotational Properties of 21 Sc Galaxies with a Large Range of Luminosities and Radii from NGC 4605 (R = 4kpc) to UGC 2885 (R = 122 kpc) *Astrophys. J.* **238** 471
[12] Yahalom A 2019 The effect of retardation on galactic rotation curves *J. Phys.: Conf. Ser.* **1239** 012006
[13] Yahalom A 2018 Retardation Effects in Electromagnetism and Gravitation *Proceedings of the Material Technologies and Modeling the Tenth International Conference, Ariel University, Ariel, Israel* arXiv: 1507.02897v2
[14] Yahalom A D M 2019 Dark Matter: Reality or a Relativistic Illusion? *Proceedings of Eighteenth Israeli-Russian Bi-National Workshop 2019, Ein Bokek, Israel* pp 17–22
[15] Wagman M 2019 Retardation theory in galaxies *Ph.D. Thesis* Senate of Ariel University, Samria, Israel
[16] Wagman M, Horwitz L P and Yahalom A 2023 Applying retardation theory to galaxies *J. Phys.: Conf. Ser.* **2482** 012005
[17] Yahalom A and (Lorentz Symmetry Group) 1693 Retardation, intergalactic mass depletion and mechanisms leading to galactic rotation curves *Symmetry* **2020** 12
[18] Yahalom A 2021 Effects of higher order retarded gravity *Universe* **7** 207
[19] Yahalom A 2021 The cosmological decrease of galactic density and the induced retarded gravity effect on rotation curves. proceedings of IARD 2020 *J. Phys.: Conf. Ser.* **1956** 012002
[20] Yahalom A 2021 Lensing effects in retarded gravity *Symmetry* **13** 1062
[21] Tully R B and Fisher J R 1977 A new method of determining distances to galaxies *Astronomy and Astrophysics.* **54** 661–73
[22] Yahalom A 2021 Tully—fisher relations and retardation theory for galaxies *Int. J. Mod. Phys.* D **30** 2142008
[23] Yahalom A 2022 Lensing effects in galactic retarded gravity: why dark matter is the same for both gravitational lensing and rotation curves *IJMPD* **31** 2242018
[24] Navarro J F, Frenk C S and White S D M 1996 The structure of cold dark matter halos *The Astrophysical Journal.* **462** 563–75
[25] Sancisi R 2003 The visible matter—dark matter coupling proceedings of IAU Symposium 220 *Dark Matter in Galaxies* ed S Ryder *et al* (Publ. Astron. Soc. Pac.) arXiv:astro-ph/0311348
[26] Milgrom M 1983 *Astrophys. J.* **270** 371
[27] Mannheim P D 1993 *Astrophys. J.* **419** 150
[28] Mannheim P D 1996 *Found. Phys.* **26** 1683
[29] Moffat J W 2006 Scalar-tensor-vector gravity theory *Journal of Cosmology and Astroparticle Physics.* **2006** 4
[30] Yahalom A 2023 MOND & retarded gravity accepted by bulgarian *Journal of Physics* **50** 1–16
[31] Yahalom A 2022 The weak field approximation of general relativity, retardation, and the problem of precession of the perihelion for mercury *Proceedings of the International Conference: COSMOLOGY ON SMALL SCALES 2022 Dark Energy and the Local Hubble Expansion Problem, Prague, September 21-24, 2022* ed M Krizek and Y V Dumin (Institute of Mathematics, Czech Academy of Sciences)
[32] Yahalom A 2023 The weak field approximation of general relativity and the problem of precession of the perihelion for mercury *Symmetry* **15** 39
[33] Landau L D L 1975 *The Classical Theory of Fields* IVth edn (Pergamon)
[34] Schwinger Julian L L and DeRaad K W Jr 1998 Classical electrodynamics *Advanced Book Program* (Perseus Books)
[35] Jackson J D 1999 *Classical Electrodynamics* IIIrd edn (Wiley)
[36] Yahalom A 2008 The geometrical meaning of time *Found. Phys.* **38** 489–97
[37] Yahalom A 2009 The gravitational origin of the distinction between space and time *Int. J. Mod. Phys.* D **18** 2155–8
[38] Abbott B P *et al* 2016 *Phys. Rev. Lett.* **116** 061102
[39] Nobel Prize A 1993 *Press Release The Royal Swedish Academy of Sciences* (The Royal Swedish Academy of Sciences)
[40] Castelvecchi D and Witze W 2016 Einstein's gravitational waves found at last *Nature News* (https://doi.org/10.1038/nature.2016.19361)
[41] Feynman R P, Leighton R B and Sands M L 2011 *Feynman Lectures on Physics* (Basic Books)
[42] Yahalom A 2018 *Proceedings of the MMT Tenth International Conference* (Ariel University)
[43] Yahalom A 2019 *J. Phys. Conf. Ser.* **1239** 012006
[44] Eckhardt D H and Pestaña J L G 2002 *Astrophys. J. Lett.* **572** L135
[45] van der Kruit P C and Searle L 1981 *Astronomy & Astrophysics* **95** 105
[46] van der Kruit P C and Searle L 1982 *Astronomy & Astrophysics* **110** 61
[47] Mathewson D S, Ford V L and Buchhorn M 1992 *Astrophys. J. Suppl. Ser.* **81** 413
[48] Persic M and Salucci P 1995 *Astrophys. J. Suppl. Ser.* **99** 501
[49] Lelli F, McGaugh S S and Schombert J M 2016 *Astron. J* **152** 157
[50] Verheijen M 1997 *PhD Thesis*
[51] Richards E E *et al* 2018 *Mon. Not. R. Astron. Soc.* **476** 5127
[52] Wiegert T B V 2010 *PhD Thesis* University of Manitoba
[53] Corbelli E 2003 *Mon. Not. R. Astron. Soc.* **342** 199–207
[54] Regan M W and Vogel S N 1994 *Astrophys. J.* **434** 536
[55] Kent S M 1987 *Astron. J* **93** 816

[56] McGaugh S 2008 *Astrophys. J.* **683** 137
[57] Portinari L, Sommer-Larsen J and Tantalo R 2004 *Mon. Not. R. Astron. Soc.* **347** 691
[58] Kennicutt R C Jr., Tamblyn P and Congdon C E 1994 *Astrophys. J.* **435** 22
[59] Fabian A 2012 *Annu. Rev. Astron. Astrophys.* **50** 455
[60] Martin C L 1999 *Astrophys. J.* **513** 156
[61] Woo J H, Son D and Rakshit S 2020 *Astrophys. J.* **901** 66
[62] McGaugh, S McGaugh's Data Pages NP, 2017 http://astroweb.case.edu/ssm/data/ (accessed on 22 January 2017)
[63] Binney J and Tremaine S 1987 *Galactic Dynamics* (Princeton University Press)
[64] Veilleux S, Cecil G and Bland-Hawthorn J 2005 *Annu. Rev. Astron. Astrophys.* **43** 769
[65] Sancisi R, Fraternali F, Oosterloo T and van der Hulst T 2008 *The Astronomy and Astrophysics Review* **15** 189
[66] McQuinn M 2016 *Annu. Rev. Astron. Astrophys.* **54** 313
[67] Martin C L 2005 *Astrophys. J.* **621** 227
[68] Heckman T M, Lehnert M D, Strickland D K and Armus L 2000 *Astrophys. J. Suppl. Ser.* **129** 493
[69] Rupke D, Veilleux S and Sanders D 2005 *Astrophys. J. Suppl. Ser.* **160** 115
[70] Strickland D K and Heckman T M 2009 *Astrophys. J.* **697** 2030
[71] Kereš D, Katz N, Weinberg D H and Davé R 2005 *Mon. Not. R. Astron. Soc.* **363** 2
[72] Tumlinson J and Fang T 2005 *Astrophys. J.* **623** L97
[73] Mac Low M-M and McCray R 1988 *Astrophys. J.* **321** 776
[74] Wang J *et al* 2014 *Astrophys. J.* **781** 55
[75] Feruglio C *et al* 2015 *Astronomy & Astrophysics* **583** A99
[76] Davé R and Oppenheimer B D 2006 *Mon. Not. R. Astron. Soc.* **374** 427
[77] Brinks E 1990 Astrophysics and space science library *The Interstellar Medium in Galaxies* vol 161 ed J M S Harley and A Thronson Jr (Springer-Science Business Media) pp 39–67
[78] Swaters R A, Sancisi R, van Albada T S and van der Hulst J M 2009 *A&A* **493** 871
[79] Zhoolideh Haghighi M H and Rahvar S 2017 *Mon. Not. R. Astron. Soc.* **468** 4048